Cluster isomerization induced by electron attachment

Dafna Scharf and Joshua Jortner

School of Chemistry, Raymond and Beverly Sackler Faculty of Exact Sciences, Tel Aviv University, 69 978 Tel-Aviv, Israel

Uzi Landman

School of Physics, Georgia Institute of Technology, Atlanta, Georgia 30332

In this paper we explore the mechanisms of cluster isomerization induced by electron attachment to small, neutral Na_4Cl_4 clusters, with the localization of an excess electron inducing structural configurational changes within the cluster. The constant temperature quantum path integral molecular dynamics method was applied to obtain information of the structure and energetics of the cluster as well as the binding energy and the charge distribution of the excess electron for $Na_4Cl_4^-$ clusters, over the temperature range of 50–1200 K. The attachment of an excess electron to the ionic cluster induced two types of configurational modifications, which can be traced to the role of the excess electron as a pseudonegative ion and to the partial neutralization of a single cation by the excess electron. Consequently, the induction of isomerization at moderately low temperatures, in conjunction with the appearance of new nuclear configurations of the negative cluster, which have no counterpart in the neutral parent cluster, are exhibited.

I. INTRODUCTION

Characteristic to small clusters is the possibility of structural isomerizations,[1-3] exhibiting themselves as transformations between distinct nuclear configurations. While at zero temperature a cluster of a given size and chemical composition has a unique structure often specified in terms of a point group symmetry, at finite temperatures an equilibrium between the accessible isomers is established. The thermodynamic occurrence probabilities (weights) of the different isomers are governed by energy and entropy differences. The rates of transformations between the isomeric forms are dictated, in addition, by dynamic factors. The ability to distinguish and characterize distinct isomers depends on the cluster size, on the nature of the interactions, and on the temperature. Small clusters ($n \leqslant 10$) may possess a small number of stable, distinguishable isomers. Upon increasing the cluster size, the number of possible, relatively stable isomers proliferates rapidly, and the free-energy differences and potential energy barriers between the isomers decrease. Consequently, the transformation rates between isomers increase such that it becomes impossible to characterize the system as residing in any one particular state for a sufficiently long time to allow such characterization. We term[3] as melting the transition of a cluster from a state of equilibrium between a discrete number of isomers to a state characterized by a continuous distribution of configurations, accompanied by a coexistence between ordered and disordered structures. For a small cluster melting may be regarded as synonymous with a stage characterized by fast isomerization between several distinct nuclear configurations. In this context ionic clusters are of particular interest since their structures are more sharply characterized (energetically) than those of van der Waals and rare gas clusters,[4] and thus operationally it is easier to investigate structural and phase transformations in these systems.

We have recently[3] explored isomerization and melting in neutral $(NaCl)_n$ clusters for $n = 4$, 16, and 108, employing classical molecular dynamics simulations. In particular, we have investigated the dynamics of isomerization from a 3D cube to a 2D ring in a $(NaCl)_4$ cluster, and have established diagnostic criteria, on the basis of physical observables such as specific heats, radial distribution functions, coordination numbers, and densities of states to distinguish between isomerization and melting.

An alternative approach to the interesting problem of configurational changes in clusters involves cluster isomerization induced by electron attachment. When a nonreactive attachment of an excess electron to a cluster results in a localized state, which has no parentage in the atomic (or molecular) states of the individual cluster constituents, the cluster nuclear structure may undergo substantial reorganization. In a recent work[5] we have established the occurrence of cluster isomerization induced by electron attachment in the small positive alkali halide $M_5Cl_4^+$ cluster (M is the alkali metal ion), where the localization of an excess electron induced a configurational change, leading to a close-energy isomer.

In this paper we explore the new mechanism of cluster isomerization induced by electron attachment to small neutral alkali-halide clusters focusing on:

(1) structures, energetics and excess electron charge distribution of isomers induced by electron attachment, which are realized over a broad temperature domain;

(2) the nature of configurational modifications induced by electron attachment;

(3) a comparison between the thermal isomerization and isomerization induced by electron attachment to the same cluster;

(4) symmetry breaking effects pertaining to nuclear configuration and to the excess electron charge distribution

induced by electron attachment to a cluster at high temperatures.

Apart from the intrinsic interest in the phenomena of cluster configurational reorganization induced by electron attachment, the alkali-halide clusters were chosen for this study because of three reasons. Firstly, the interionic interactions in these systems are well understood.[1,5,6] Secondly, substantial information exists[1,5] for both neutral and charged clusters of this family. Thirdly, extensive information is available[6] on electron-alkali atom and electron-halide anion pseudopotentials.

We have studied electron attachment to the neutral Na_4Cl_4 cluster by the constant-temperature quantum path integral molecular dynamics (QUPID) method.[5] Using this method we obtained information on the structure, energetics, and excess electron charge distribution of $Na_4Cl_4^-$ clusters over the temperature domain 50 to 1200 K. The QUPID computer simulations, which rest on a discrete version of the Feynman path integral method,[7] provide a powerful approach for the exploration of excess electron states in clusters.[5,8] Furthermore, our recent model calculations[6] on electron attachment to alkali halide molecules inspire confidence in the applicability of the QUPID method in conjunction with the appropriate pseudopotentials for the study of electron attachment to alkali-halide clusters.

II. METHODOLOGY

The quantum path integral molecular dynamics (QUPID) method was applied to a system of an electron interacting with a Na_4Cl_4 cluster. Assuming pair interactions, the Hamiltonian of the system is

$$H = K + V + K_e + V_e, \qquad (2.1)$$

where K is the kinetic energy operator of the N-ion cluster with masses M_I;

$$K = -\sum_{I=1}^{N} \frac{\hbar^2}{2M_I} \nabla_I^2, \qquad (2.2)$$

V is the interionic potential energy operator of the N-ion cluster

$$V = \frac{1}{2} \sum_{I=1}^{N} \sum_{J=1}^{N} {}' \Phi_{IJ}(R_{IJ}), \qquad (2.3)$$

K_e is the kinetic energy of the electron (mass m)

$$K_e = -\frac{\hbar^2}{2m} \nabla^2, \qquad (2.4)$$

and V_e is the operator for the potential energy of the electron which consists of a sum of the electron-ion interaction potential

$$V_e = \sum_{I=1}^{N} \Phi_{eI}(\mathbf{r} - \mathbf{R}_I). \qquad (2.5)$$

The partition function Z of the system is given by

$$Z = \mathrm{Tr}\, \exp(-\beta H), \qquad (2.6)$$

where $\beta = 1/k_B T$ is the inverse temperature. An approximate expression for the partition function can be obtained through the use of Trotter's formula[9] to replace the sum of operators in the exponent by a product of P terms,

$$Z_P = \mathrm{Tr}\left[\exp\left(-\frac{\beta K}{P}\right) \exp\left(-\frac{\beta V}{P}\right) \right.$$
$$\left. \times \exp\left(-\frac{\beta K_e}{P}\right) \exp\left(-\frac{\beta V_e}{P}\right) \right]^P \qquad (2.7)$$

and

$$Z = \lim_{P \to \infty} Z_P.$$

Using the expression for the free particle propagator in the coordinate representation, Z_P can be written as

$$Z_P = \left(\frac{mP}{2\pi\hbar^2\beta} \right)^{3P/2} \prod_I^N \left(\frac{M_I P}{2\pi\hbar^2\beta} \right)^{3P/2}$$
$$\times \int \exp[-\beta(V_{\mathrm{eff}}^e + V_{\mathrm{eff}}^I)]d\tau, \qquad (2.8)$$

where the effective potential for the electron is

$$V_{\mathrm{eff}}^e = \sum_{i=1}^{P} \left[\frac{Pm}{2\hbar^2\beta^2}(\mathbf{r}_i - \mathbf{r}_{i+1})^2 + \frac{V_e(r)}{P} \right] \qquad (2.9)$$

and it is understood here that $\mathbf{r}_{(P+1)} \equiv \mathbf{r}_1$. The effective potential for the ions is given by

$$V_{\mathrm{eff}}^I = \sum_i^P \left[\sum_I^N \frac{PM_I}{2\hbar^2\beta^2}(\mathbf{R}_{iI} - \mathbf{R}_{(i+1)I})^2 + \frac{V}{P} \right] \qquad (2.10)$$

and the integration in Eq. (2.8) is taken over the volume

$$d\tau = d^3R_1 \cdots d^3R_P\, d^3r_1 \cdots d^3r_P.$$

When $M_I \gg m$, the thermal wavelength of the ions $(\beta\hbar^2/M_I)^{1/2}$ is much smaller than that of the electron and the Gaussian functions corresponding to the heavy atoms reduce to δ functions. The resulting expression for the partition function is

$$Z_P = \prod_{I=1}^{N} \left(\frac{M_I P}{2\pi\beta\hbar^2} \right)^{3P/2} \left(\frac{mP}{2\pi\beta\hbar^2} \right)^{3P/2} \int \exp\{-\beta V_{\mathrm{eff}}\}d\tau, \qquad (2.11)$$

where

$$V_{\mathrm{eff}} = V_{\mathrm{eff}}^e + V. \qquad (2.12)$$

This result reflects the frequently used approximation that in a system consisting of a light particle and interacting with heavier ones, the heavy particles can be treated using classical mechanics, whereas a quantum treatment is required for the light particle.

Equations (2.9) and (2.11) establish an approximate isomorphism between the quantum problem and a corresponding classical one.[10] In the isomorphic classical problem, the electron is mapped onto a closed chain (necklace) of P pseudoclassical particles (beads) with nearest-neighbor harmonic interactions whose strength is determined by the mass (m), the inverse temperature (β), and the number of beads (P). The average energy of the system can then be evaluated from the relation

$$\langle E \rangle = -\frac{\partial}{\partial\beta} \ln Z = \frac{3N}{2\beta} + \langle V \rangle + K_e + \frac{1}{P}\left\langle \sum_{i=1}^{P} V_e(\mathbf{r}_i) \right\rangle, \qquad (2.13)$$

where the pointed brackets indicate averages over the Boltzmann distribution as defined in Eq. (2.8). The electron kinetic energy estimator is

$$K'_e = \frac{3P}{2\beta} - \frac{Pm}{2\hbar^2\beta^2}\left\langle\sum_{i=1}^{P}(\mathbf{r}_i - \mathbf{r}_{i+1})^2\right\rangle. \tag{2.14a}$$

An alternative expression for K_e can be obtained[11] in the form

$$K_e = \frac{3}{2\beta} + \frac{1}{2P}\sum_{i=1}^{P}\left\langle\frac{\partial V_e(\mathbf{r}_i)}{\partial \mathbf{r}_i}\cdot(\mathbf{r}_i - \mathbf{r}_P)\right\rangle. \tag{2.14b}$$

The first term on the rhs of Eq. (2.14b) is the free particle contribution K_{free} and the second term K_{int} is the contribution from the interaction, with the ions.

The averages over the Boltzmann distribution can be replaced by phase-space trajectories generated by an effective Hamiltonian to be discussed in Sec. III.

III. NUMERICAL METHOD

The calculations were performed for a model of an electron attached to a cluster of Na_4Cl_4. The Na^+ and Cl^- ions, which were treated classically, were taken to interact through a Born–Mayer potential,

$$\Phi_{IJ}(R_{IJ}) = A_{IJ}\exp\{-R_{IJ}/\rho_{IJ}\} + \frac{Z_IZ_Je^2}{R_{IJ}}. \tag{3.1}$$

The potential parameters were those determined by Fumi and Tosi.[12]

The electron–anion interaction was modeled[6] by a Coulomb repulsion from the closed-shell anion, complemented by the electron induced polarization interaction, which is operative at distances larger than the ionic radius R_I of the Cl^- ion, and is corrected for the "self-energy of the induced dipole,"

$$\Phi_{eI} = \frac{1}{P}\sum_{i=1}^{P}\left(\frac{e^2}{r_{iI}} - \frac{e^2\alpha_I}{2r_{iI}^4}\right), \quad r_{iI} \geqslant R_I$$

$$= \frac{1}{P}\sum_{i=1}^{P}\frac{e^2}{r_{iI}}, \quad r_{iI} < R_I. \tag{3.2}$$

The local pseudopotential for the electron–cation interaction was taken[13,14] as

$$\Phi_{eI} = -\frac{e^2}{r_{iI}}, \quad r_{iI} > R_C$$

$$= -\frac{e^2}{R_C}, \quad r_{iI} \leqslant R_C, \tag{3.3}$$

where R_C is a cutoff parameter ($R_C = 3.26\,a_0$ for Na^+) and r_{iI} is the distance between the ith bead and the Ith ion.

The statistical sampling over the Boltzmann distribution was replaced by the equivalent[15] averaging over the phase-space trajectories. The trajectories were generated via classical MD by the Hamiltonian

$$H = \sum_{i=1}^{P}\frac{m^*\dot{\mathbf{r}}_i^2}{2} + \sum_{i=1}^{N}\frac{M_I\dot{\mathbf{R}}_I^2}{2}$$

$$+ \sum_{i=1}^{P}\left[\frac{Pm}{2\hbar^2\beta}(\mathbf{r}_i - \mathbf{r}_{i+1})^2 + \frac{1}{P}V_e\right] + V, \tag{3.4}$$

where the masses m^* and M_I can be chosen to be arbitrary, since in classical systems configurational averages do not depend on the masses appearing in the kinetic energy term.

In our calculations we choose $m^* = 1$ amu and M_I to be the ionic masses. This choice is made such that the internal frequencies of the quantum necklace $\omega \sim [mP/m^*\beta^2\hbar^2]^{1/2}$ will match the frequencies of the nuclear motion.

In order to study the temperature effect on the equilibrium configuration, we have utilized a constant-temperature version of MD[16] where the particles are subjected to stochastic collisions. The equations-of-motion were integrated using the velocity form of the Verlet algorithm.[16]

In the initial configuration of the system the electron-bead particles were randomly distributed over a sphere of radius R_s, centered about the ionic cluster. R_s was chosen to be 15 times the crystalline lattice constant of NaCl, being of the order of the thermal wavelength of a free electron at high temperatures ($T \sim 1000$ K). The ionic cluster was set initially in a cubic configuration.

The initial run [2000–2500 integration steps, Δt, with a time unit (tu) of 1.03×10^{-15} s] during which the system was subjected to frequent rescaling of the velocities using a fifth-order predictor–corrector integration algorithm and a small integration time step of $\Delta t = 0.01$ units, allowed for a slow approach of the electron bead particles towards the ions. Subsequently, the system was equilibrated applying the constant-temperature procedure with the Verlet algorithm. Typical values which we used for the stochastic collision frequency (STCF) were: STCF (ions) $\sim 1 \times 10^{-3}$ collisions per particle per unit integration step; STCF (electron beads) $\sim 1 \times 10^{-4}$ in the same units. The lengths of the equilibration stage for different temperatures and the corresponding integration steps are given in Table I. Averaging was then performed over the subsequent integration steps as indicated in Table I. The number of integration steps was carefully chosen to ensure proper sampling of the phase space and reliable averaging. We have further found that a large number of integration steps ($\sim 10^5$ time units) is required in the equilibration stage before the physical quantities and their standard deviations converge, especially so since the system can undergo considerable configurational changes.

IV. RESULTS

We have investigated the equilibrium characteristics of an electron attached to a cluster of Na_4Cl_4 at four temperatures: 50, 575, 750, and 1000 K. We have found that different equilibrium configurations were exhibited for $Na_4Cl_4^-$ as a

TABLE I. The numerical parameters of the QUPID simulations at various temperatures: T is the temperature in K; P is the number of electron beads; Δt is the integration time step in units of 1.03×10^{-15} s; N_{eq} is the number of integration steps in the equilibration stage; N_{av} is the number of integration steps over which averages were calculated in the averaging stage.

T(K)	P	Δt	N_{eq}	N_{av}
50	1000	2	50 000	50 000
575	520	1	100 000	100 000
750	520	0.3	135 000	100 000
1000	250	0.25	160 000	210 000

function of temperature (Figs. 1 to 3). Three temperature domains can be distinguished:

(1) The low temperature domain $0 < T < 500$ K. From calculations at 50 and 350 K we find that the localization of the electron in this low temperature range is exhibited mainly inside the cubic equilibrium configuration of the ions [Fig. 1(a)], which is very similar to the low-temperature configuration of the neutral Na_4Cl_4 cluster,[3] which will be discussed in Sec. V. Accordingly, no major configurational changes are exhibited in the ionic cluster.

(2) The intermediate temperature domain 500 K $< T < 750$ K. In this range a configurational change of the negative charged cluster is exhibited. At a temperature of ~ 575 K the cluster with the attached electron shows a single configuration, which resembles an open umbrella, with the electron beads at one of the corners [Fig. 1(b)] with the ionic cluster being in a distorted planar configuration.

(3) The high temperature domain 750 K $< T < 1200$ K. In this range coexistence of several isomers of Na_4Cl_4 prevails. At ~ 750 K a boat-like configuration of the cluster with the electron bead in the center [Fig. 2(a)] and a bent-chain configuration [Fig. 2(b)] dominate. At
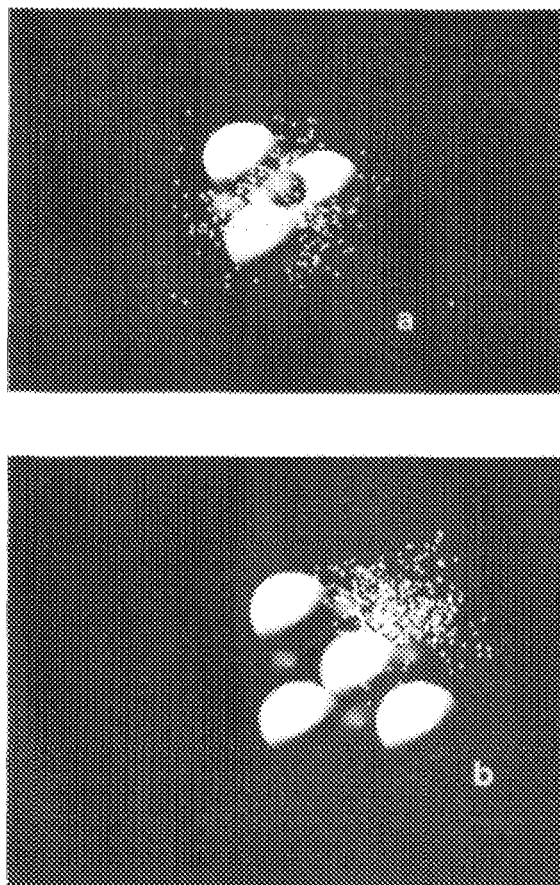

FIG. 2. Configurations of $Na_4Cl_4 + e^-$ at 750 K. For details see caption of Fig. 1.

FIG. 1. Configurations of $Na_4Cl_4 + e^-$ at 50 K (a) and 575 K (b). The large bright spheres and small dark spheres represent the Cl^- and Na^+ ions (the sizes were scaled according to the corresponding ionic radii). The small dots are the locations of the quantum pseudoparticles (beads), representing the excess electron charge distribution. Note in the configuration shown in (b) the excess electron occupies the position of a halide anion in the $(Na_4Cl_4)Cl^-$ cluster (see Fig. 6).

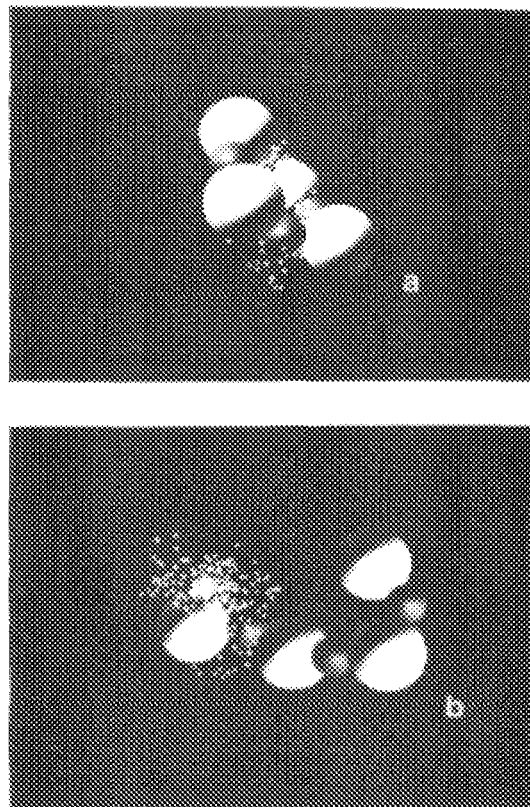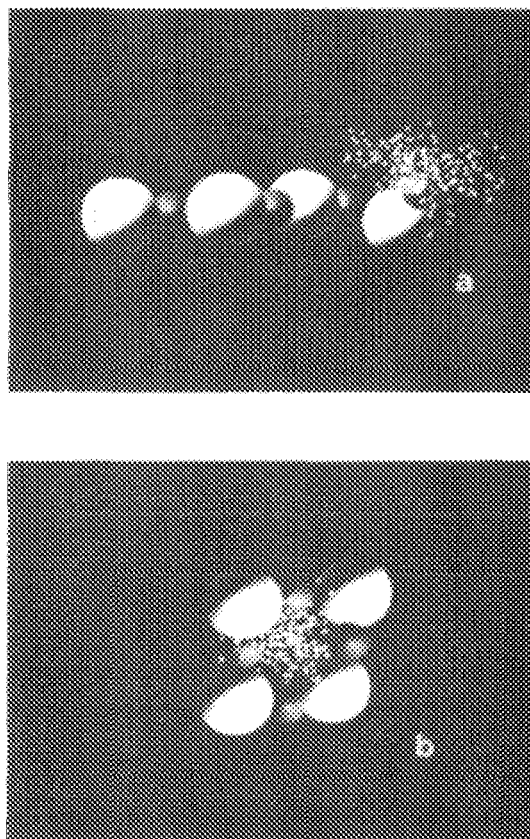FIG. 3. Configurations of $Na_4Cl_4 + e^-$ at 1000 K. For details see caption of Fig. 1.

TABLE II. Energetics of the ionic systems as a function of temperature. The potential energy (PE_{ions}), kinetic energy (KE_{ions}), and the total energy (E_{ions}) for the neutral and the negatively charged systems are given in a.u. (hartree). The standard deviations are given in parentheses.

Na_4Cl_4		50 K	575 K	750 K	1000 K
	PE_{ions}	− 1.025 84	− 1.026 32	− 1.026 56	− 1.026 33
		(1×10^{-6})	(1×10^{-6})	(1×10^{-6})	(1×10^{-6})
	KE_{ions}	1.43×10^{-3}	1.62×10^{-2}	2.16×10^{-2}	2.86×10^{-2}
		(1×10^{-6})	(1×10^{-6})	(1×10^{-6})	(1×10^{-6})
	E_{ions}	− 1.024 40	− 1.010 08	− 1.004 96	− 0.997 76
		(1×10^{-6})	(1×10^{-6})	(1×10^{-6})	(1×10^{-6})
$Na_4Cl_4^-$					
	PE_{ions}	− 0.979	− 0.95	− 0.94	− 0.91
		(0.005)	(0.01)	(0.02)	(0.03)
	KE_{ions}	0.002	0.024	0.028	0.04
		(6×10^{-4})	(0.007)	(0.008)	(0.01)
	E_{ions}	− 0.977	− 0.93	− 0.91	− 0.87
		(0.006)	(0.01)	(0.02)	(0.03)

~ 1000 K an elongated chain isomer [Fig. 3(a)] is encountered in coexistence with a planar ring configuration [Fig. 3(b)].

The energetics of the cluster is given in Tables II and III. In Table II we have listed the energies of the ionic cluster for the neutral, parent, Na_4Cl_4 cluster, as well as the energies of the classical ions in the negatively charged $Na_4Cl_4^-$ cluster. The ionic potential energies PE_{ions} were calculated according to Eq. (3.1). The total energies of the ionic cluster, E_{ions}, are given by the sum

$$E_{ions} = PE_{ions} + KE_{ions}. \tag{4.1}$$

In Table III we present the calculated energies of the electron bead particles and the total energy of the negatively charged cluster. The electron potential energy PE_{elec} was calculated according to Eq. (2.5) using Eqs. (3.2) and (3.3) for the potential.

The kinetic energy of the electron was calculated by two methods. First, using the estimator of Eq. (2.14b) for K_e and, second, using Eq. (2.14a) for K'_e. We have found that both estimators and their corresponding standard deviations

converge to the same values. However, the estimator based on the derivative of the potential energy of the electron–ion interactions, Eq. (2.14b), tends to converge faster.

The total energy of the electron E_{elec} is

$$E_{elec} = PE_{elec} + K_e. \tag{4.2}$$

The total energy of the $Na_4Cl_4^-$ cluster was calculated by using the sum of the total energies of the ions and of the electron,

$$QE = PE_{ions} + KE_{ions} + PE_{elec} + K_{int} + K_{free}. \tag{4.3}$$

The electron affinity (EA) of Na_4Cl_4 can be calculated from the difference between the total energies of the charged cluster (QE in Table III) and of the neutral parent cluster (E_{ions} for Na_4Cl_4 in Table II) at low temperatures, where the entropy contribution can safely be neglected. The value of the electron affinity of Na_4Cl_4 is EA = (0.029 ± 0.008) hartree, or (0.8 ± 0.2) eV. This electron affinity is considerably lower than the EA of large positive ionic clusters.[5]

In Table IV we list the relevant characteristics of the electron charge distribution:

(a) The average distance between the center of mass of the electron bead and the center of mass of the ions is given by

$$D_{CM} = \left\langle \left| \frac{1}{P} \sum_{i=1}^{P} \mathbf{r}_i - \frac{\Sigma_I M_I \mathbf{R}_I}{\Sigma_I M_I} \right| \right\rangle. \tag{4.4}$$

The occurrence of a substantial configurational change in the charged cluster, when going from the low temperature domain to the intermediate and high temperature regions can easily be inferred from the D_{CM} values at the various temperatures (Table IV). At the low temperature domain, where the ionic cluster remains in the cubic conformation, the centers of mass of the ions and electron-bead distribution almost coincide and equal penetrations of the electron bead to within the cutoff radius of the four sodium cations are found. Already at 575 K, the distance between the centers of mass becomes large. The relatively small standard deviation for D_{CM} reflects the presence of a single configuration at intermediate temperatures. At the high temperature domain D_{CM} is again large, being characterized by large standard

TABLE III. Energetics of the electron bead and total energy of $Na_4Cl_4^-$ at various temperatures. PE_{elec} is the electron potential energy; K_e is the electron kinetic energy estimator according to Eq. (2.14b); K'_e is the electron kinetic energy estimator according to Eq. (2.14a), E_{elec} is the total energy of the electron, and QE is the total energy of $Na_4Cl_4^-$. All the energies are in a. u. (hartree); standard deviations are given in parentheses.

	50 K	575 K	750 K	1000 K
PE_{elec}	− 0.146	− 0.13	− 0.14	− 0.15
	(8×10^{-3})	(2×10^{-2})	(2×10^{-2})	(3×10^{-2})
K'_e	7.0×10^{-2}	6×10^{-2}	6×10^{-2}	6×10^{-2}
	(7×10^{-3})	(1×10^{-2})	(1×10^{-2})	(2×10^{-2})
K_e	7×10^{-2}	6×10^{-2}	6×10^{-2}	6×10^{-2}
	(7×10^{-3})	(1×10^{-3})	(1×10^{-2})	(1×10^{-2})
E_{elec}	− 0.076	− 0.07	− 0.08	− 0.09
	(8×10^{-3})	(2×10^{-2})	(2×10^{-2})	(3×10^{-2})
QE	− 1.053	− 1.004	− 0.99	− 0.96
	(8×10^{-3})	(2×10^{-2})	(2×10^{-2})	(3×10^{-2})

TABLE IV. Configurational characteristics of $Na_4Cl_4^-$. D_{CM} is the distance between the centers of mass of the electron bead distribution and the ions. R_g is the radius of gyration of the electron necklace. The thermal wavelength for a free electron is denoted by λ_T [Eq. (4.6)] and that calculated via Eq. (4.7) is denoted by λ_T (calc). QC is the fraction of the quantum contribution to the kinetic energy of the electron bead. $\mathcal{R}/\mathcal{R}_f$ is the ratio between the breadth of the localized electron necklace and a free particle. All quantities are in a.u. (hartree and bohr radii).

	50 K	575 K	750 K	1000 K
D_{CM}	0.4 ± 0.2	6 ± 1	5 ± 2	4 ± 3
R_g	4.2 ± 0.2	4.9 ± 0.5	4.8 ± 0.5	4.5 ± 0.6
λ_T(calc)	67.6	22.5	20.2	17.3
λ_T	79.7	23.7	20.8	17.9
QC	99%	95%	93%	90%
$\mathcal{R}/\mathcal{R}_f$	0.09	0.33	0.39	0.42

deviations. These large standard deviations in the averaged distance between the centers of mass reflect the coexistence of several configurations contributing to the equilibrium state. We have indeed confirmed the occurrence of isomerization at these high temperatures where ring-like configurations which are characterized by relatively small D_{CM} (~ 1 a_0), coexist with open chain (bent or elongated) configurations where D_{CM} is relatively large (~ 5–15 a_0). These configurations can be further characterized by low penetration ratios of the electron charge distribution to within the cutoff radius (R_C) of the cations. While in the low temperature domain up to 75% of the electron bead particles were found within R_C of the four cations, only 40% of the electron bead particles were located within the cutoff radius of the cations at 575, 750, and 1000 K. Moreover, in the elevated temperature domain, the configurations involve penetration of the electron bead to one or two cations, while equal penetration to all four cations is exhibited in the low temperature domain.

(b) The radius of gyration of the electron bead is given by the second moment with respect to the center of mass

$$R_g = \left[\frac{1}{2P^2} \left\langle \sum_{i,j=1}^{P} (\mathbf{r}_i - \mathbf{r}_j)^2 \right\rangle \right]^{1/2}. \quad (4.5)$$

The gyration radius is a measure of the spatial extent of the wave packet of the excess electron. It is evident that the size of the electron, at different temperatures, does not change significantly (Table IV).

(c) The thermal wavelength of a free electron is given by

$$\lambda_T = (\beta \hbar^2/m)^{1/2}. \quad (4.6)$$

We may define[17] a quantity λ_T (calc) as

$$\lambda_T(\text{calc}) = \left[\frac{P}{P-1} \left\langle \sum_{i=1}^{P} (\mathbf{r}_i - \mathbf{r}_{i+1})^2 \right\rangle \right]^{1/2}. \quad (4.7)$$

For a free electron λ_T (calc) $= \lambda_T$. From the results in Table IV we observe that the thermal wavelength of the electron (as defined above) is not influenced significantly by the interaction with the ionic system.

(d) The quantum character of the excess electron, defined by

$$QC = K_{int}/(K_{int} + K_{free}) \quad (4.8)$$

is obviously large, decreasing slightly at higher temperatures.

(e) The extent of the localization of the excess electron relative to a free electron can be inferred from the self-pair-correlation function in the (imaginary) time domain[18]:

$$\mathcal{R}^2(t-t') = \langle |\mathbf{r}(t) - \mathbf{r}(t')|^2 \rangle; \quad 0 \leqslant t - t' \leqslant \beta \hbar, \quad (4.9)$$

where $|\mathbf{r}(t) - \mathbf{r}(t')|$ is the distance between two points (beads) on the electron path separated by a "time" $(t - t')$ within the interval $(0, \beta \hbar)$. The characteristic breadth of the electron distribution is given by $\mathcal{R} = \mathcal{R}(\beta \hbar/2)$. While for a free particle $\mathcal{R}(\beta \hbar/2) = \sqrt{3}\lambda_T$, a localized electron is characterized by a relatively tight spatial distribution of the beads and therefore would exhibit $\mathcal{R}(\beta \hbar/2) < \lambda_T$. Hence, a measure of the electron localization is given by the ratio $\mathcal{R}(\beta \hbar/2)/\sqrt{3}\lambda_T$, which is denoted by $\mathcal{R}/\mathcal{R}_f$ in Table IV and which was found to be significantly smaller than unity. Thus, the electron is well localized at all the temperatures which were studied by us.

V. DISCUSSION

Electron attachment may induce configurational transformations in small neutral ionic clusters at relatively low temperatures. The equilibrium configurations of the cluster with the attached electron do not necessarily relate to the equilibrium configurations of the parent neutral cluster. Detailed molecular dynamics simulations of the temperature effect on the equilibrium configuration of the neutral Na_4Cl_4 cluster[3] show that for $T < 700$ K, only a single cubic conformation is stable [see Figs. 4(a) and 5]. Within the range 700 K $< T < 875$ K the neutral cluster exhibits coexistence of a cube and a ring isomer, while in the temperature range 875 K $< T < 1250$ K only the ring isomer is stable [see Figs. 4(b)
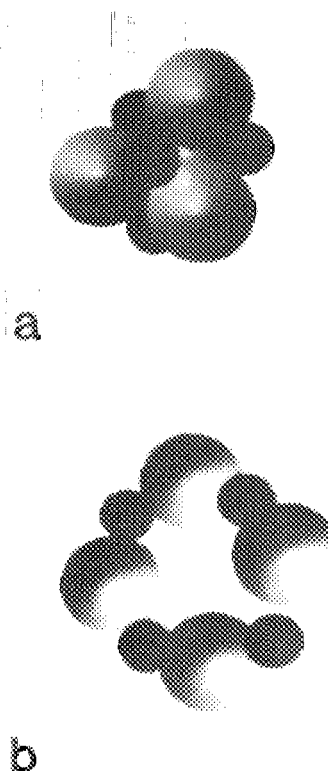

FIG. 4. Configurations of Na_4Cl_4 at $T < 700$ K (a) and at $T > 700$ K (b). Note the similarity between the cubic configuration in (a) and the low temperature configuration of $Na_4Cl_4^-$ [Fig. 1(a)].
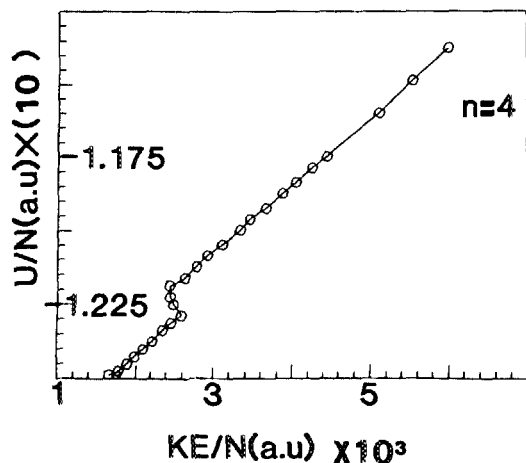
FIG. 5. Caloric curve (total energy per particle, U/N, vs kinetic energy per particle, KE/N, for Na_4Cl_4). The break at $T = 700$ K corresponds to the isomerization transition between the low temperature, cube, and high temperature, ring isomers (see Fig. 4).

and 5]. At temperatures above 1250 K, the ring coexists with an open chain isomer up to ~ 1400 K, where evaporation processes set in. The caloric curve (total energy per particle vs kinetic energy) shown[3] in Fig. 5 exhibits the isomerization transition as a break at $T \approx 700$ K.

The presence of the excess electron in the ionic cluster induces two types of configurational modifications in $Na_4Cl_4^-$ which are either quantitatively or qualitatively different from those in the neutral Na_4Cl_4 cluster:

(i) The localized excess electron can play the role of a pseudonegative ion with appreciable kinetic energy, which is overwhelmed by the potential energy of the electron in the field of the ions. Consequently, new nuclear configurations of the negative cluster, which have no counterpart in the neutral cluster, will be exhibited.

(ii) Partial neutralization of a single cation by the excess electron results in the appearance of the high-temperature configuration of the neutral parent cluster at substantially lower temperatures for the negatively charged cluster (compare Figs. 2 and 3 with Figs. 4 and 5).

Effect (i) is observed in the intermediate temperature range, while both effects (i) and (ii) are exhibited in the high temperature domain. Consider first the low and intermediate temperature domains. For the neutral cluster, the onset of the first isomerization transition, cube (3D) $\rightarrow$ ring (2D), which is exhibited at ~ 700 K (see Fig. 5) appears already at ~ 550 K for $Na_4Cl_4^-$ [Fig. 1(b)]. The $Na_4Cl_4^-$ cluster with the attached electron exhibits a distorted planar configuration, which is drastically different from its low temperature configuration. Moreover, this planar configuration of an open umbrella of the $Na_4Cl_4^-$ differs from any known equilibrium configuration of the parent neutral Na_4Cl_4 cluster at any temperature. It is interesting to note that a similar umbrella-type configuration was found at all temperatures for the related $Na_4Cl_5^-$ cluster over the temperature range 50 K $< T <$ 1300 K which was explored by MD simulations (see the Appendix). Proceeding to the high temperature behavior of the Na_4Cl_4 and $Na_4Cl_4^-$ clusters, we have found[3]

that for Na_4Cl_4 the ring (2D) $\rightarrow$ chain (1D) transition is exhibited only at ~ 1250 K, while for $Na_4Cl_4^-$ we have encountered already at 750 K the isomerization of the boat configuration (3D) to an open, bent worm-like configuration [Fig. 2(b)]. At 1000 K the "boat" configuration of $Na_4Cl_4^-$ becomes planar [Fig. 3(b)] and the chain is elongated [Fig. 3(a)].

The comparison between the energetics of the ions in the parent neutral Na_4Cl_4 cluster and in the charged $Na_4Cl_4^-$ cluster (Table II) clearly demonstrates the existence of substantial higher total energies in the charged system at all temperatures. Three effects add up to this overall increase of the total ionic energy: (a) The partial neutralization of the cations by the excess electron, which somewhat screens the positive charges and results in a higher potential energy of the ions in the charged cluster relative to that of the parent neutral cluster. (b) Small configurational modifications of the ionic structure of $Na_4Cl_4^-$ relative to that of Na_4Cl_4, while preserving the approximate cubic structure at low temperatures, increase both the potential and the kinetic energy of the ions (Table II). (c) Configurational relaxation which breaks the cubic structure of $Na_4Cl_4^-$ at intermediate and high temperatures and which is distinct from the behavior of the neutral cluster, results in major modifications of the ionic potential energy upon electron attachment.

A general trend of lowering the total energy at higher temperatures is exhibited by both charged and neutral clusters. However, the difference between the ionic cluster reorganization energy E_c, i.e., the difference between the total ionic energy of the neutral and the charged clusters

$$E_c = E_{ions}(Na_4Cl_4^-) - E_{ions}(Na_4Cl_4) \qquad (5.1)$$

becomes larger at higher temperatures. ($E_c \sim 1.5$ eV at 50 K and increasing to $E_c \sim 3$ eV at 1000 K). Since the total energy of the attached electron (E_{elec} in Table III) does not vary appreciably and the ionic energy increases at higher T, the total energy QE of the charged cluster increases at higher temperatures.
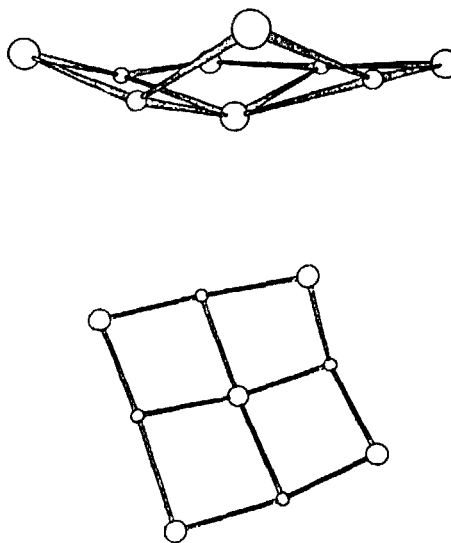

FIG. 6. The stable, umbrella-shaped configuration of $(Na_4Cl_4)Cl^-$, obtained via simulations in the temperature range 50–1000 K, shown from two different perspectives.

TABLE V. Energetics of the $Na_4Cl_5^-$ as a function of temperature: PE is the potential energy, KE is the kinetic energy, and E is the total energy. Energies in a.u. (hartree). Standard deviations are given in parentheses.

$Na_4Cl_5^-$:	50 K	575 K	750 K	1000 K
PE	-1.1082	-1.0810	-1.1087	-1.1062
	(3×10^{-4})	(4×10^{-4})	(3×10^{-4})	(9×10^{-4})
KE	1.7×10^{-3}	1.97×10^{-2}	2.51×10^{-2}	3.45×10^{-2}
	(3×10^{-4})	(4×10^{-4})	(3×10^{-4})	(9×10^{-4})
E	-1.1065	-1.0884	-1.0836	-1.072
	(4×10^{-4})	(5×10^{-4})	(4×10^{-4})	(1×10^{-3})

The variations in the charge distribution associated with the excess electron with temperature, reflect a "transition" from a relatively extended electronic state at low T to a localized electronic state at high T. In the extended state (at 50 K) the excess electron is spread with equal probability over the four Na^+ ions. In contrast, the localized state observed at elevated temperatures exhibits electron localization around a single cation. It is likely that at the low temperature domain, symmetry considerations dominate and determine the mode of localization of the excess electron. Symmetry breaking effects, induced by the cluster vibrational excitations, prevail at the intermediate and high temperature domains, resulting in configurational changes and in localization of the electron around one (or two) Na^+ ions.

ACKNOWLEDGMENTS

APPENDIX

In our classical molecular dynamics simulations of the system $(NaCl)_4 Cl^-$ the interionic interactions were those given in Eq. (3.1). The system was equilibrated for 3×10^5 time steps, $\Delta t = 0.5$ tu, (1 tu $= 1.46\times10^{-15}$ s), except for $T = 1000$ K, where the time step was 0.25 tu and 5×10^5 time steps were required to equilibrate the system. Averaging was performed over the subsequent 5×10^5 time steps.

At all the temperatures studied by us the stable structure of the systems corresponds to an umbrella-type configuration shown in Fig. 6. The energetics of the system are summarized in Table V.

[1] T. P. Martin, Phys. Rep. **95**, 169 (1983).
[2] G. Natanson, F. Amar, and R. S. Berry, J. Chem. Phys. **78**, 399 (1983).
[3] J. Luo, U. Landman, and J. Jortner, *Proceedings of the International Workshop on the Physics and Chemistry of Small Clusters*, edited by R. Khana and P. Jena (Plenum, New York, 1987).
[4] J. Jortner, D. Scharf, and U. Landman, *Proceedings of the Enrico Fermi International School of Physics on Condensed Matter Theory, 1986* (North-Holland, Amsterdam, 1987).
[5] U. Landman, D. Scharf, and J. Jortner, Phys. Rev. Lett. **54**, 1860 (1985).
[6] D. Scharf, J. Jortner, and U. Landman, Chem. Phys. Lett. **130**, 504 (1986), and references cited therein.
[7] R. P. Feynman and A. R. Hibbs, *Quantum Mechanics and Path Integrals* (McGraw-Hill, New York, 1965).
[8] U. Landman, R. N. Barnett, C. L. Cleveland, D. Scharf, and J. Jortner, *Proceedings of the International Symposium on the Physics and Chemistry of Small Clusters*, edited by R. Khana and P. Jena (Plenum, New York, 1987); J. Phys. Chem. (in press).
[9] L. S. Schulman, *Techniques and Applications of Path Integrals* (Wiley, New York, 1981).
[10] D. Chandler and P. G. Wolynes, J. Chem. Phys. **79**, 4078 (1981); D. Chandler, J. Phys. Chem. **88**, 3400 (1984).
[11] M. F. Herman, E. J. Bruskin, and B. J. Berne, J. Chem. Phys. **76**, 5150 (1982).
[12] F. G. Fumi and M. P. Tosi, J. Phys. Chem. Solids **25**, 31, 45 (1964).
[13] J. V. Abarenkov and V. Heine, Philos. Mag. **12**, 529 (1965).
[14] R. W. Shaw, Phys. Rev. **174**, 769 (1968).
[15] M. Parrinello and A. Rahman, J. Chem. Phys. **80**, 86 (1984).
[16] J. R. Fox and H. C. Anderson, J. Phys. Chem. **88**, 4019 (1984).
[17] B. De Raedt, H. Sprik, and N. L. Klein, Chem. Phys. **80**, 5719 (1984).
[18] A. L. Nichols, D. Chandler, V. Singh, and D. M. Richardson, J. Chem. Phys. **81**, 5109 (1984).